Experimental Demonstration of the Time Reversal Aharonov-Casher Effect

doi: 10.1103/PhysRevLett.97.196803

Experimental Demonstration of the Time Reversal Aharonov-Casher Effect

Tobias Bergsten,[1,3] Toshiyuki Kobayashi,[1] Yoshiaki Sekine,[1] and Junsaku Nitta[1,2,3]

[1]*NTT Basic Research Labs, 3-1 Morinosato-Wakamiya, Atsugi-shi, Kanagawa 243-0198, Japan*

[2]*Graduate School of Engineering, Tohoku University, 6-6-02 Aramaki-Aza Aoba, Aoba-ku, Sendai 980-8579, Japan*

[3]*CREST-Japan Science and Technology Agency, Kawaguchi Center Building, 4-1-8, Hon-cho, Kawaguchi-shi, Saitama 332-0012, Japan*

(Received 12 December 2005; published 8 November 2006)

We demonstrate the time reversal Aharonov-Casher (AC) effect in small arrays of mesoscopic semiconductor rings. By using an electrostatic gate we can control the spin precession rate and follow the AC phase over several interference periods. We show that we control the precession rate in two different gate voltage ranges; in the lower range the gate voltage dependence is strong and linear and in the higher range the dependence in almost an order of magnitude weaker. We also see the second harmonic of the AC interference, oscillating with half the period. We finally map the AC phase to the spin-orbit interaction parameter α and find it is consistent with Shubnikov–de Haas analysis.

DOI: 10.1103/PhysRevLett.97.196803 PACS numbers: 85.35.Ds, 71.70.Ej, 73.23.−b

Spintronics is the art of generating, manipulating, and detecting the spin of electrons in solid state electronic devices. While this has traditionally involved ferromagnetic materials and external magnetic fields, we can also manipulate spins with purely electric fields via the spin-orbit interaction (SOI) between a moving spin particle and an electric field. In particular, we can design a semiconductor heterostructure with a two-dimensional electron gas (2DEG) which has an internal electric field perpendicular to the 2DEG due to an asymmetric quantum well. We will then have SOI even without external electric fields. This is called the Rashba effect [1,2].

The SOI is a relativistic effect on a particle with spin which is moving through an electric field. In the particle's frame of reference there will be a magnetic field perpendicular to the electric field and the direction of movement. The spin direction will precess around the axis parallel to this magnetic field and the precession rate depends on the spin-orbit interaction strength α ($\Delta = 2\alpha k_F$, Δ is the spin splitting energy), and the value of α can be controlled by a gate voltage [3]. This allows us to control the spin precession rate with an electrostatic gate on top of the heterostructure.

In this Letter we present evidence of quantum interference effects due to spin precession in small arrays of mesoscopic 2DEG rings. This interference is an Aharonov-Casher (AC) effect [4] of time reversal symmetric paths and is the electromagnetic dual [5] to the Al'tshuler-Aronov-Spivak (AAS) effect [6]. Previously the AC effect has been detected in a neutron interferometry experiment [7]. As the AAS effect and the related Aharonov-Bohm (AB) effect have proven to be important tools in research, we can expect that the AC effect will be a powerful tool for understanding quantum interactions and material properties. We further show that we can control the spin precession rate with an electrostatic gate and modulate the interference pattern over several periods. Earlier experiments on square loop arrays yielded similar results, but only for up to one interference period [8]. We also see the second order AC effect where the oscillation period is half the period of the first order effect and the oscillations correspond to up to 26π spin precession angle. Second and third order harmonics have also recently been observed in square loop arrays [9]. We map the interference pattern to changes in α and combine the results with measurements of α using Shubnikov–de Haas (SdH) beating patterns, which are consistent with the spin interference data. Other related experiments include single rings which gave inconclusive results [10], and Aharonov-Bohm type AC effect in a single ring with a complex gate voltage dependence [11].

The ring arrays were etched out in a dry-etching process from an InAlAs/InGaAs based 2DEG (Fig. 1), similar to sample 1 in Ref. [12]. The electron mobility was 7–11 m^2/Vs depending on the carrier density and the effective electron mass m^* was $0.050m_e$ as determined from the temperature dependence of SdH oscillations. By using arrays rather than single rings we get a stronger signal and we average out some of the universal conduc-

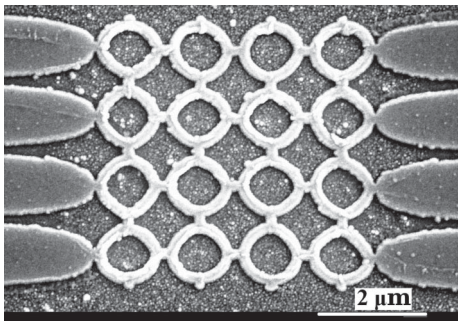

FIG. 1. An SEM image of an array of 0.5 μm radius rings. The array is covered by a 50 nm SiO_2 insulator layer and an 80 nm Au gate. The width of the rings is 100 nm after dry etching.

tance fluctuations (UCF) and AB oscillations [13]. The arrays consisted of between 3×3 and 6×6 rings. The (average) radius of the rings was between 0.5 and 1.1 μm and the width was 20% of the radius. The rings were covered with a 50 nm thick SiO_2 insulator layer, deposited by ECR sputtering, and on top of that was an Au gate, used to control the carrier density and the SOI strength α. The advantage of using a small number of rings rather than a large array is that the gate leakage is much smaller and we can use relatively high gate voltage. This makes it possible to see several oscillations of AC interference.

Close to the arrays and in the same current path and under the same gate was a Hall bar, 5 μm wide and 20 μm long, used to measure the carrier density. For the SdH measurements we used a larger Hall bar, 20 μm by 120 μm, covered by an identical gate structure.

The resistance of a mesoscopic ring is affected by several quantum interference effects. The well-known AB effect results in a resistance oscillation with a magnetic flux period of h/e. Another is the AAS effect, which works in parallel with the AB effect and occurs when the two wave function parts travel a full turn around the ring in opposite directions and interfere at the entry point. Contrary to the AB effect, the two parts follow the exact same path but in different directions, or time reversal symmetric paths. This means that it is independent of the Fermi momentum (and consequently the carrier density) and the interference is always constructive in the absence of magnetic flux. However, the AAS effect is sensitive to the spin phase (the AC phase) as we show in this Letter. When the flux is increased the resistance oscillates with the period $h/2e$, but the amplitude decays after a few periods because of averaging between different paths in the ring, with different areas.

In Fig. 2 we display the resistance versus magnetic field for an array of rings. In the top graph we can see both

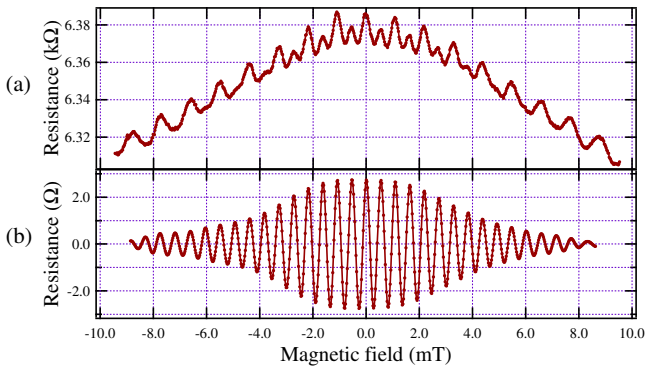

FIG. 2 (color online). The resistance of an array of rings vs the magnetic field. The array consisted of 4×4 rings with 1.1 μm radius. (a) Raw data, averaged from eight sweeps with slightly different gate voltages (1.9–2.0 V). (b) The same data after going through a digital band-pass filter, showing the $h/2e$ oscillations clearly with the amplitude falling off with higher field.

interference effects described above. The fast oscillations near the center are the $h/2e$ oscillations and the slower are the h/e oscillations which do not decay significantly at higher magnetic fields [14]. The background peak is most likely due to weak localization. In our experiments we are interested in the $h/2e$ oscillations and in order to see them more clearly we feed the raw data through a digital band-pass filter [15] (bandwidth approximately 40% of the peak frequency), as shown in the lower graph.

If there is SOI in the ring, the electron spin will start precessing around the effective magnetic field. The precession axes for the two parts of the wave function are opposite and therefore the relative precession angle is twice the angle of each part. Depending on this angle the interference is constructive or destructive, and in the case of destructive interference the phase of the $h/2e$ oscillations will shift by π, which we interpret as negative amplitude.

In the following, precession angle (rate) refers to the precession of a single path.

The precession angle of an electron moving along a straight narrow channel is $\theta_0 = 2\alpha m^* L/\hbar^2$, where L is the distance travelled [16]. In a ring the precession is a bit more complicated because of the precession axis constantly changing direction. The $h/2e$ oscillation amplitude can be written as [17–19]

$$\frac{\delta R_\alpha}{\delta R_{\alpha=0}} = \cos\left[2\pi\sqrt{1+\left(\frac{2\alpha m^*}{\hbar^2} r\right)^2}\right], \qquad (1)$$

with δR_α and $\delta R_{\alpha=0}$ being the $h/2e$ oscillation amplitude with and without SOI, respectively, and r the radius of the ring. In the limit of strong SOI or large rings the argument of the cosine reduces to θ_0 because the distance travelled around the ring is $2\pi r$.

The experiment was carried out in a ^{3}He cryostat at the base temperature which varied between 220 and 270 mK. The sample was in the core of a superconducting magnet with the field B perpendicular to the 2DEG plane. We measured the resistance R of the ring array simultaneously with the Hall resistance R_H of the Hall bar close to the rings, while stepping the magnetic field and the gate voltage V_G. Figure 3 shows the result after digital band-pass filtering of the $h/2e$ oscillations which are visible as vertical bands in the figure. We can clearly see the oscillations switching phase as we increase the gate voltage.

In order to reduce noise and UCF effects we averaged ten resistance versus magnetic field (R versus B) curves with slightly different gate voltages. This averaging preserves the $h/2e$ oscillations but the averaging of M curves reduces the h/e oscillation amplitude roughly as $M^{-1/2}$ [10,20].

We calculated the $h/2e$ oscillation amplitude by integration of the $h/2e$ peak of the FFT spectra of R versus B curves. We then plotted the amplitude against the gate voltage. Figure 4 shows the results from three different

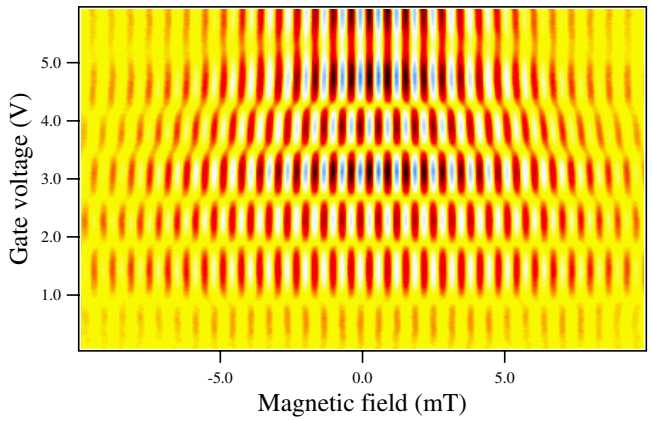

FIG. 3 (color online). The resistance vs gate voltage and magnetic field after digital filtering [see Fig. 2(b)]. Color scale is black-red-yellow-white-blue. We clearly see the $h/2e$ oscillations switching phase as the gate voltage is increased. The sample is a 5×5 array of 1.0 μm radius rings.

ring arrays. We also calculated the carrier density n_e from the slope of the R_H versus B ($n_e^{-1} = edR_H/dB$) and plotted it in the same diagrams. It was important to measure n_e simultaneously with R rather than measuring the n_e versus V_G dependence separately because the dependence shifted considerably between different gate voltage sweeps. This is obvious from Fig. 4(a) and 4(b) which are measured on arrays with the same ring radius, 1.0 μm. All the features

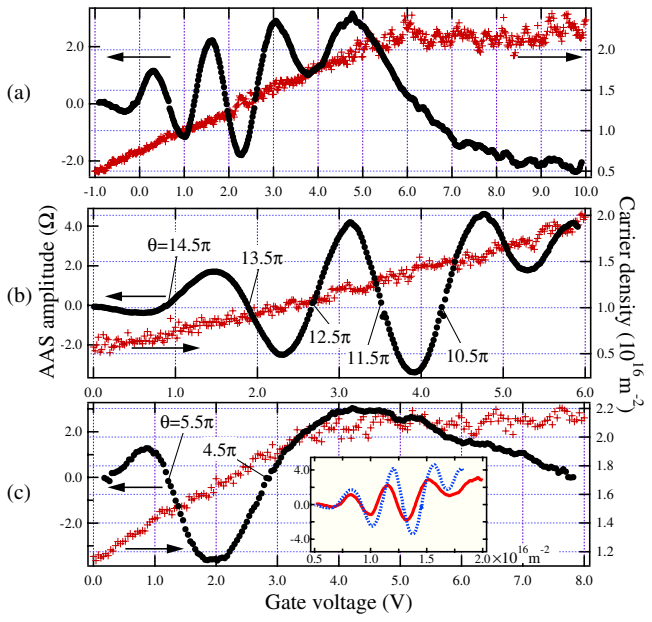

FIG. 4 (color online). The time reversal AC effect. $h/2e$ (AAS) oscillation amplitude and carrier density plotted against the gate voltage for three different ring arrays: (a) 3×3 array, 1.0 μm radius; (b) 5×5 array, 1.0 μm; (c) 6×6 array, 0.5 μm. Inset of (c): the amplitudes of (a) [solid lines] and (b) [dotted lines] plotted against the carrier density. The precession angle θ corresponds to the argument of the cosine in Eq. (1).

of graph (b) are faithfully reproduced in graph (a), except it is shifted by about 1 V. If we plot the amplitude against the carrier density instead [inset of Fig. 4(c)] we see that the two curves agree very well.

As we see in Fig. 4 the $h/2e$ amplitude oscillates as we change the carrier concentration using the top gate. As the gate voltage is changed, the SOI strength α changes with it and as we expect from Eq. (1) the $h/2e$ amplitude crosses zero, inverting the $h/2e$ oscillations. Each period represents one extra 2π spin precession of an electron moving around a ring. However, the top two graphs have an unexpected "half oscillation" (a negative peak which does not cross zero) at a carrier concentration of 1.7×10^{16} m^{-2}. There is no theoretical explanation for this result. We also notice from the top and bottom graphs that the carrier density saturates around 2.2×10^{16} m^{-2}, and that the $h/2e$ amplitude is still changing, but much more slowly.

Since we are measuring the electron density in a Hall bar rather than in the rings directly, there may be some difference due to depletion of the 2DEG near the edges. However, the fact that the density in the Hall bar saturates at about the same voltage as where the oscillations in the rings slow down indicates that the difference is small.

In the FFT spectra there is also a small peak at $h/4e$. This is due to the wave function parts going twice around the ring before interfering. We may also have interference from paths going around two neighboring rings, with the same period, but we do not know the amplitude of this contribution. We expect, however, that the period is 8 times longer with respect to V_G [21], and thus longer than our measurement range. If we do the same analysis on this peak we get an oscillating amplitude with half the period compared to the $h/2e$ amplitude (Fig. 5). This is expected because the distance is twice and therefore the precession angle is also twice. The first peak we can distinguish from the noise, at 2.3 V, corresponds to a precession angle of 26π. In the $h/4e$ curve the negative peaks correspond to the zero crossings of the first harmonic, while the positive peaks correspond to the peaks, positive and negative. The amplitudes of the $h/4e$ oscillations are between 40 and 100

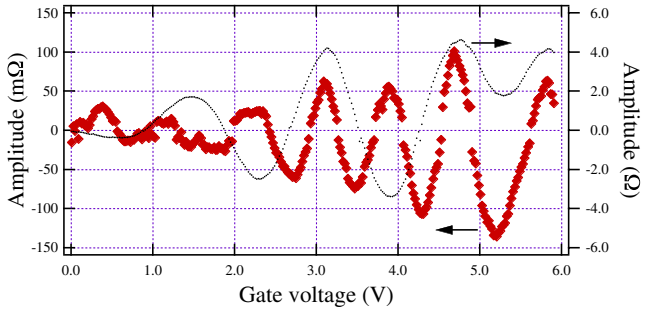

FIG. 5 (color online). The $h/4e$ amplitude ($\diamond$) oscillates with half the period compared to the $h/2e$ amplitude ($\bullet$). These data are from the same measurement as Fig. 4(b).

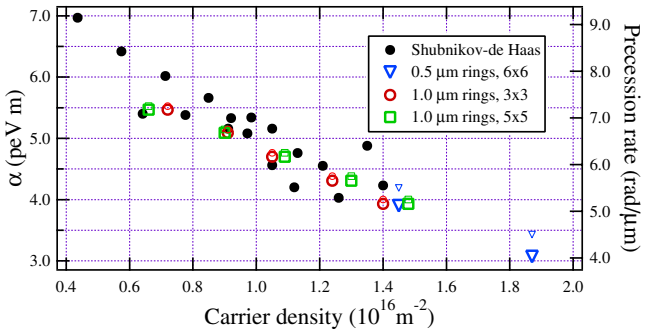

FIG. 6 (color online). By combining α values derived from Shubnikov–de Haas measurements (●) and from the zero crossings of the spin interference graphs (□, ○, and ▽) we can map α values over a wide range of carrier densities. The right axis shows the corresponding precession rates $\theta_0/2\pi r$. The small symbols are the actual precession rates in the rings [the argument of the cosine in Eq. (1)] which are slightly higher, particularly for the 0.5 μm rings.

times smaller than the $h/2e$ oscillations, depending on the gate voltage. Since the amplitude decreases exponentially with the electron path length [13] we can write the ratio of the amplitudes as $A_{h/2e}/A_{h/4e} = \exp[(4\pi r - 2\pi r)/L_\phi]$, which gives a coherence length L_ϕ between 1.4 and 1.7 μm. We note one interesting point: the negative peak at 5.2 V in the $h/4e$ curve corresponds to the "half oscillation" in the first harmonic rather than a zero crossing.

We can use the oscillations to map α against n_e, like in Ref. [8]. According to Eq. (1) the $h/2e$ amplitude is zero when

$$\alpha = \pm \frac{\hbar^2}{8m^* r}\sqrt{(2N+1)^2 - 16}, \qquad (2)$$

with integer $N > 1$. The zero crossings in the graphs correspond to consecutive values of N. However, this does not tell us the absolute value of α, so we measured beatings in SdH oscillations in order to anchor the string of zero crossings to an absolute value [22].

We measured SdH oscillations at different carrier densities in a separate Hall bar and calculated α from the beating patterns (black dots in Fig. 6). We know from similar heterostructures that the value of α is positive [12]. Now we can map the spin interference graphs to absolute α values by choosing suitable values of N, see Fig. 6. The gate voltage sensitivity $\Delta\alpha/\Delta V_G$ is 0.46–0.57 peV m/V in the range below carrier density saturation. In the saturation region the sensitivity is much smaller, 0.05–0.11 peV m/V.

To conclude, we have shown that the spin precession rate can be controlled in a precise and predictable way with an electrostatic gate. We have experimentally demonstrated the time reversal AC effect, the electromagnetic dual to the AAS effect, in small arrays of rings, including the second harmonic of this effect. Our spin interference data agree with SdH measurements of α. The precise spin precession control is important in order to realize semiconductor spintronics devices based on SOI, e.g., the Datta-Das transistor [16].

[1] E. I. Rashba, Fiz. Tverd. Tela (Leningrad) **2**, 1224 (1960) [Sov. Phys. Solid State **2**, 1109 (1960)].
[2] Y. A. Bychkov and E. I. Rashba, J. Phys. C **17**, 6039 (1984).
[3] J. Nitta, T. Akazaki, H. Takayanagi, and T. Enoki, Phys. Rev. Lett. **78**, 1335 (1997).
[4] Y. Aharonov and A. Casher, Phys. Rev. Lett. **53**, 319 (1984).
[5] H. Mathur and A. D. Stone, Phys. Rev. Lett. **68**, 2964 (1992).
[6] B. L. Al'tshuler, A. G. Aronov, and B. Z. Spivak, Pis'ma Zh. Eksp. Teor. Fiz. **33**, 101 (1981) [JETP Lett. **33**, 94 (1981)].
[7] A. Cimmino, G. I. Opat, A. G. Klein, H. Kaiser, S. A. Werner, M. Arif, and R. Clothier, Phys. Rev. Lett. **63**, 380 (1989).
[8] T. Koga, Y. Sekine, and J. Nitta, Phys. Rev. B **74**, 041302 (2006).
[9] Y. Sekine, T. Koga, and J. Nitta (to be published).
[10] J. Nitta, T. Koga, and H. Takayanagi, Physica (Amsterdam) **12E**, 753 (2002).
[11] M. König, A. Tschetschetkin, E. M. Hankiewicz, J. Sinova, V. Hock, V. Daumer, M. Schäfer, C. R. Becker, H. Buhmann, and L. W. Molenkamp, Phys. Rev. Lett. **96**, 076804 (2006).
[12] T. Koga, J. Nitta, T. Akazaki, and H. Takayanagi, Phys. Rev. Lett. **89**, 046801 (2002).
[13] C. P. Umbach, C. Van Haesendonck, R. B. Laibowitz, S. Washburn, and R. A. Webb, Phys. Rev. Lett. **56**, 386 (1986).
[14] A. D. Stone and Y. Imry, Phys. Rev. Lett. **56**, 189 (1986).
[15] The digital filter used was the *Digital FIR Filter.vi*, included in LabVIEW from National Instruments. It implements the Remez/Parks-McClellan algorithm; for details, see, e.g., T. W. Parks and J. J. McClellan, IEEE Trans. Circuits Syst. **19**, 189 (1972).
[16] S. Datta and B. Das, Appl. Phys. Lett. **56**, 665 (1990).
[17] J. Nitta, F. E. Meijer, and H. Takayanagi, Appl. Phys. Lett. **75**, 695 (1999).
[18] D. Frustaglia and K. Richter, Phys. Rev. B **69**, 235310 (2004).
[19] M. J. van Veenhuizen, T. Koga, and J. Nitta, Phys. Rev. B **73**, 235315 (2006).
[20] A. F. Morpurgo, J. P. Heida, T. M. Klapwijk, B. J. van Wees, and G. Borghs, Phys. Rev. Lett. **80**, 1050 (1998).
[21] M. J. van Veenhuizen (private communication).
[22] Th. Schäpers, G. Engels, J. Lange, Th. Klocke, M. Hollfelder, and H. Lüth, J. Appl. Phys. **83**, 4324 (1998).